

NEW DESIGN OF SSR2 SPOKE CAVITY FOR PIP II SRF LINAC*

P. Berrutti[†], I. Gonin, T. N. Khabiboulline, M. Parise, D. Passarelli, G. Romanov, F. Ruiiu, A. Sukhanov, V. Yakovlev, Fermilab, Batavia, IL 60510, USA

Abstract

Superconducting SSR2 spoke cavities provide acceleration of the H- in PIP II SRF linac from 35 to 185 MeV. The RF and mechanical design of the SSR2 cavities has been completed and satisfies the technical requirements. However, our recent results of the high RF power tests of fully dressed SSR1 cavities show considerably strong multipacting (MP), which took significant time to process. On the other hand, the new results of the tests of balloon cavity showed significant mitigation of MP. In this paper we present the results of the improved design of the SSR2 cavity, based on the balloon cavity concept. The electromagnetic design is presented, including RF parameter optimization, MP simulations, field asymmetry analysis, High Order Mode (HOM) calculations. Mechanical analysis of the dressed cavity is presented also, which includes Lorentz Force Detuning (LFD) optimization, and reduction of the cavity resonance frequency sensitivity versus He pressure fluctuations. The design completely satisfies the PIP II technical requirements.

INTRODUCTION

PIP-II stands for Proton Improvement Plan-II [1]: it is Fermilab plan for future improvements to the accelerator complex, aimed at providing LBNE (Long Base Neutrino Experiment) operations with a beam power of at least 1 MW on target. The central element of the PIP-II is a new superconducting linac, injecting into the existing Booster. The PIP-II 800 MeV linac derives from Project X Stage 1 design. The room temperature (RT) section includes a Low Energy Beam Transport (LEBT), RFQ and Medium Energy Beam Transport (MEBT), accelerating H- ions to 2.1 MeV and it creates the desired bunch structure for injection into the superconducting (SC) linac. PIP-II will use five SC cavity types: one 162.5 MHz half wave resonator (HWR), two single spoke resonator sections at 325 MHz (SSR1 and SSR2), lastly two families of 650 MHz elliptical cavities low beta (LB) and high beta (HB). The technology map of the PIP-II linac, Fig. 1, shows the transition energies between accelerating structures, and the transition in frequency.

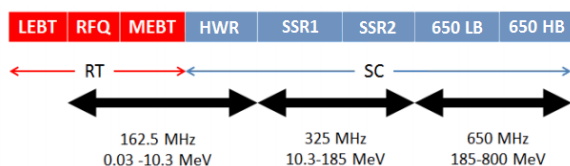


Figure 1: PIP-II linac technology map.

This article will discuss the electromagnetic (EM) design of the second type of spoke resonators (SSR2): the design has been updated again mainly to mitigate multipacting, while trying to preserve the cavity performance. The phenomenon of multipacting (MP) consists in electron multiplication at surfaces exposed to an oscillating electromagnetic field, which can represent a serious obstacle for operation of particle accelerator and their RF components. Multipacting, in the previous designs of SSR2, has been studied in [2, 3]: the results in [2] showed higher intensity and wider power range than for SSR1 cavities, already built and tested at FNAL [4, 5], results in [3] show already improved MP but yet non-negligible barriers were present in the operating gradient range. The new design presented here improves both MP intensity reduces the gradient range in which it occurs. The main modification to the cavity geometry concerns the end-walls: now they have an elliptical profile to reduce multipacting as suggested from the balloon spoke developed at TRIUMF [6, 7]. This article summarizes all the studies on SSR2 design for PIP-II: EM parameters, quadrupole field asymmetry, HOMs and multipacting simulations are presented. In addition preliminary multi-physics studies are included: LFD and df/dP have been calculated and optimized.

GEOMETRY AND RF PARAMETERS

SSR2 is a single spoke resonator operating at 325 MHz, it will be used in PIP-II linac to accelerate H- from 35 MeV to 185 MeV. Figure 2 shows the new SSR2 RF design Y-Z cross-section where Z represents the beam axis. All the main geometry parameters values are reported in Table 1. Electric and magnetic 3D fields have been simulated with CST Microwave studio and are plotted in Fig. 3.

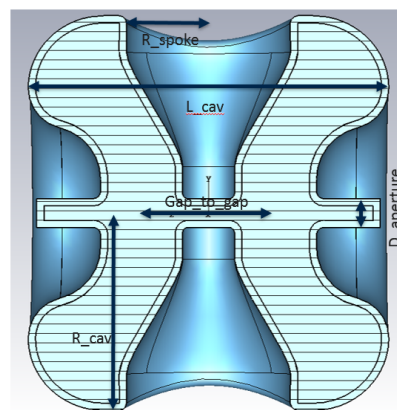


Figure 2: New SSR2 cavity Y-Z cross-section.

The value of $\beta_{opt} = 0.47$ has been chosen after optimization of the SSR2 section of PIP-II in [8]. SSR2 new design

Cavities - Design
 non-elliptical

Content from this work may be used under the terms of the CC BY 3.0 licence (© 2019). Any distribution of this work must maintain attribution to the author(s), title of the work, publisher, and DOI.

* Work supported by D.O.E. Contract No. DE-AC02-07CH11359
[†] berrutti@fnal.gov

Table 1: Main Geometric Parameters

Parameter	[mm]
L_cav	500
R_cav	273.2
R_spoke	114
D_aperture	40
Gap_to_gap	185.9

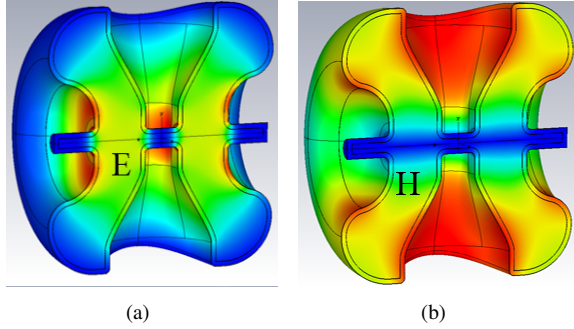


Figure 3: Electric field (a) and magnetic field (b) in SSR2 cavity.

v3.1 and previous design v2.6 EM parameters are compared in Table 2. One can see how the two designs deliver equivalent EM performance. SSR2 v3.1 has slightly higher peak surface fields, still it allowing safe operation at maximum gradient. The gradient E_{acc} is defined over the effective length $L_{eff} = \beta_{opt} \lambda$, where λ is the electromagnetic field wavelength at 325 MHz.

Table 2: SSR2 EM Parameters Design Comparison

Parameter		SSR2 v3.1	SSR2 v2.6
Frequency	[MHz]	325	325
Optimal beta β_{opt}		0.472	0.475
Effective length L_{eff}	[m]	0.436	0.438
E_{peak}/E_{acc}		3.51	3.38
B_{peak}/E_{acc}	[mT/(MV/m)]	6.75	5.93
G	[Ohm]	115	115
R/Q	[Ohm]	305	297
B_{peak} at 5 MeV	[mT]	77.4	67.7

TRANSVERSE FIELD ASYMMETRY

The lack of azimuthal symmetry in spoke resonators affects transverse electric and magnetic fields, introducing a perturbation to beam dynamic: a particle will be subject to non-uniform radial kick. This could be a potential issue since the focusing in SSR2 cryomodules relies upon solenoids, which provide uniform radial correction. Transverse field asymmetry has been studied for all PIP-II superconducting cavities [9], since the design of SSR2 has been updated it was necessary to study its transverse field perturbation. The transverse momentum gain can be calculated using the for-

mulae 1, 2, where $\beta = v/c$ is considered constant through the cavity, Z_0 is the impedance of free space and α is the angle on the x-y plane with respect to the x axis.

$$\Delta p_x(r, \alpha)c = \int_{z_i}^{z_f} \left(\frac{E_x(r, \alpha)}{\beta} - Z_0 i H_y(r, \alpha) \right) e^{i \frac{kz}{\beta}} dz \quad (1)$$

$$\Delta p_y(r, \alpha)c = \int_{z_i}^{z_f} \left(\frac{E_y(r, \alpha)}{\beta} + Z_0 i H_x(r, \alpha) \right) e^{i \frac{kz}{\beta}} dz \quad (2)$$

Since the transverse field asymmetry will induce a quadrupole kick, one can define the parameter Q , defined in Eq. (3), which is directly proportional to the quadrupole strength.

$$Q = \frac{\Delta p_x(r, 0)c - \Delta p_y(r, \pi/2)c}{(\Delta p_x(r, 0)c + \Delta p_y(r, \pi/2)c)/2}, \quad (3)$$

Figure 4 shows the difference between the transverse components of electric and magnetic fields for SSR2 cavity v2.6. Integrating the transverse fields for all the particle β between 35 and 185 MeV one can calculate the asymmetry parameter Q . Figure 5 compares the quadrupole parameter for SSR2 v2.6 and v3.1, both curves show a significant x-y asymmetry for the momentum gain. SSR2 v3.1 shows the same quadrupolar strength as SSR2 v2.6. Since the quadrupole of SSR2 v2.6 could be managed by the existing corrector design the same applies to SSR2 v3.1 field asymmetry.

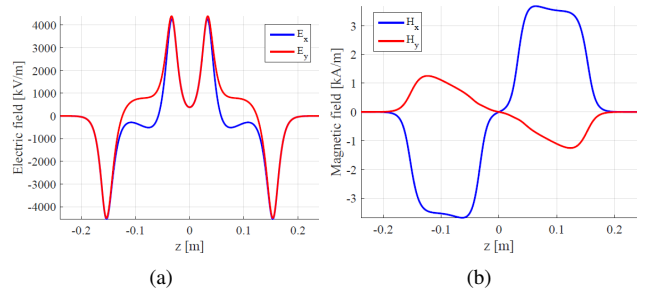


Figure 4: Transverse electric (a) and magnetic (b) fields in SSR2 v3.1 at 10 mm offset.

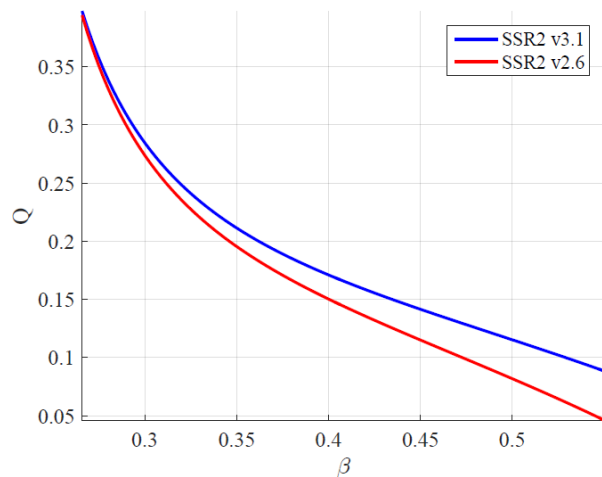


Figure 5: Q parameter vs β from 35 to 185 MeV.

MULTIPACTING MITIGATION

Particular attention has been put in the MP mitigation of SSR2 since the very beginning of the design process [2]. Then a first geometry change was implemented [3]: it consisted in adding a small step at the transition of the cylindrical shell and end-wall, as shown in Fig. 6 v2.6. An additional optimization has been carried out going to elliptical profile for the end-wall: SSR2 v3.1 also in Fig. 6. This last geometry change has been suggested from the MP results of the balloon spoke resonator built and tested at TRIUMF [6, 7].

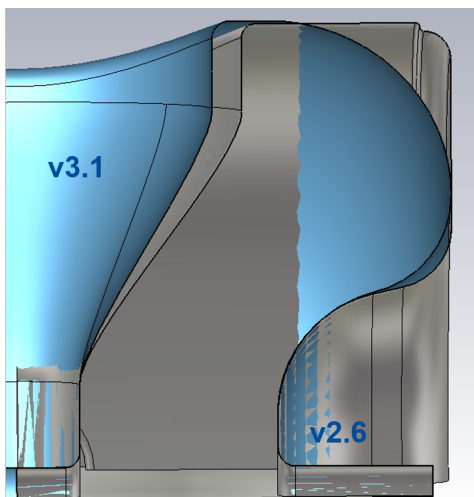


Figure 6: Difference between SSR2 v2.6 (double step) and SSR2 v3.1 (elliptical end-wall profile).

Multipacting simulations have been carried out using CST particle studio. It is crucial to enhance the mesh quality near the cavity surface since the MP develops mostly in this region; see Fig. 7. Both field levels, electric and magnetic, and particle tracking are affected by the mesh quality. CST offers various choices for Niobium secondary emission yield, in this paper only the lowest yield is considered corresponding to discharge cleaned niobium.

MP Figure of Merit

Once the cavity fields have been simulated and the electrons have been tracked for several RF periods, if MP is present, particle multiplication over time can be noticed from the plot of total number of particle vs time. A typical resonant multipacting scenario is presented in Fig. 8(a), where the number of particles is exponentially increasing with time: once the MP process is started the number of particles $N(t)$ can be written as $N(t) = N_0 e^{\alpha t}$. Given the exponential behavior of the number of particles vs time, one can define the growth rate, α , as the exponential coefficient of the particle number fit. Taking into account the last few (usually 3-4) RF periods one can calculate α as shown in Fig. 8(b).

MP Results

The new SSR2 design (v3.1) shows improved multipacting characteristics compared to the older design iteration:

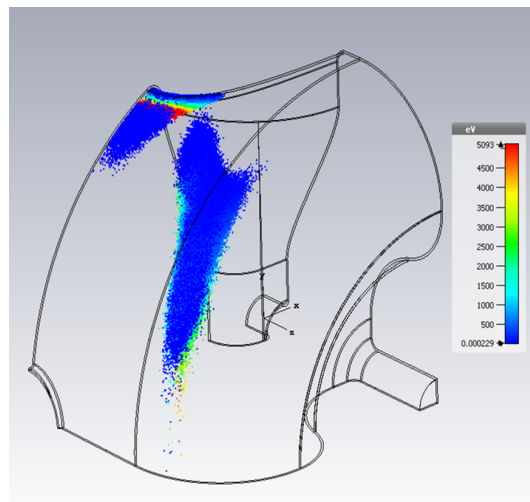


Figure 7: Electrons trajectories in SSR2 v3.1 at $V=1.24$ MV (maximum MP intensity).

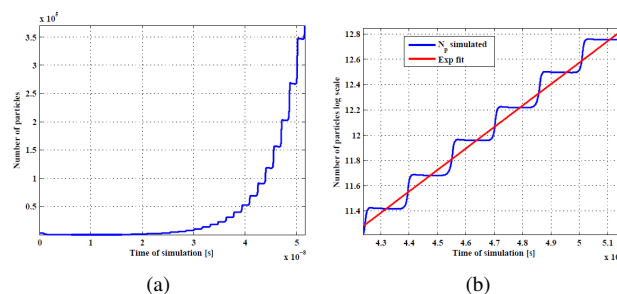


Figure 8: Particle number exponential growth (a) and growth rate, α , calculation (b).

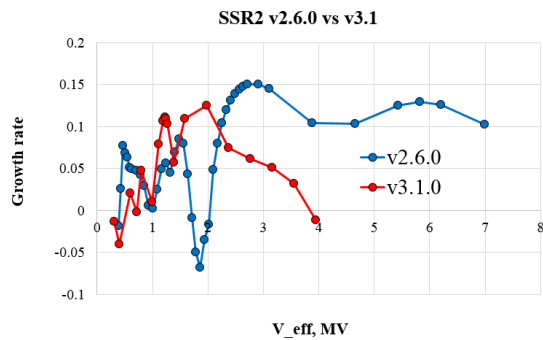
MP is not suppressed but its intensity and gradient range are reduced especially around operating voltage ($\approx 4-5$ MV). The Fig. 9 shows growth rate for both SSR2 v3.1 and v2.6 on the left. In addition, on the right of Fig. 9 SSR2 v3.1 and SSR1, already built and tested at FNAL, growth rate have been compared. The new SSR2 design has the lowest growth rate; this is a good indication that the multipacting in SSR2 v3.1 is going to be easier to overcome during cold tests.

HOMS ANALYSIS

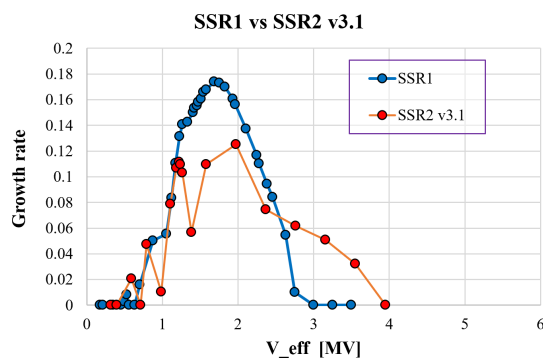
The spoke resonator geometry is complex but taking advantage of different boundary conditions one can select which kind of modes to simulate. The two transverse planes can be set to induce the Electric field continuity (E) or magnetic field continuity (M). In general, there are four main categories of mode polarizations:

- Monopoles: these modes are found with MM boundaries, like the accelerating mode they have E components on axis.
- Horizontal Dipoles: EM boundary conditions, zero E field on the vertical transverse plane.
- Vertical Dipoles: ME boundary conditions, zero E field on the horizontal transverse plane.
- Quadrupoles: EE boundaries, electric field is zero on both transverse planes, not at 45 degrees.

Content from this work may be used under the terms of the CC BY 3.0 licence (© 2019). Any distribution of this work must maintain attribution to the author(s), title of the work, publisher, and DOI.



(a)



(b)

Figure 9: Growth rate comparison from CST PIC simulations: SSR2 v3.1 and SSR2 v2.6 (a), SSR2 v3.1 and SSR1 (b).

In Fig. 10 it is represented the transverse field pattern for modes belonging to the two dipole families and quadrupoles.

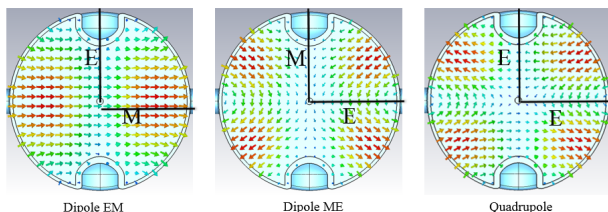


Figure 10: HOMs polarizations: horizontal dipole (left), vertical dipole (center) and quadrupole (right) field transverse pattern.

All monopole, dipole and quadrupole modes have been simulated for frequencies up to around 1 GHz. HOMs R/Q vs beta curve is calculated to understand how efficient all modes are at exchanging energy with the particles. R/Q vs β for all monopoles is plotted in Fig. 11. The first HOM shows R/Q higher than the accelerating mode in the low part of the beta range, but its frequency is not multiple of any main of the beam harmonics, so the overall energy exchange is minimal.

R/Q has been calculated at $\beta_{opt} = 0.472$ for all dipole and quadrupole modes, the results are shown in Fig. 12. SSR2 cavity is not equipped with HOMs dampers: all higher modes will be attenuated through the fundamental power coupler, Fig. 13 presents the Q_{ext} values simulated for all HOMs through the FPC antenna.

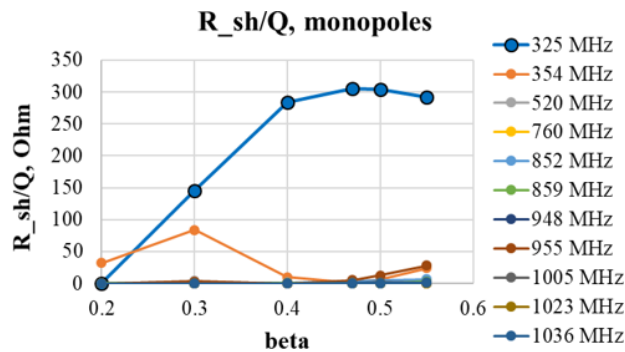


Figure 11: R/Q vs beta for all monopole modes of SSR2 cavity up to 1 GHz.

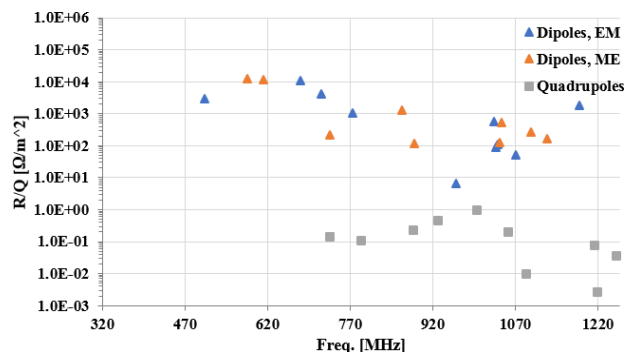


Figure 12: R/Q at beta optimal calculated for all dipole and quadrupole modes of SSR2 up to 1.2 GHz.

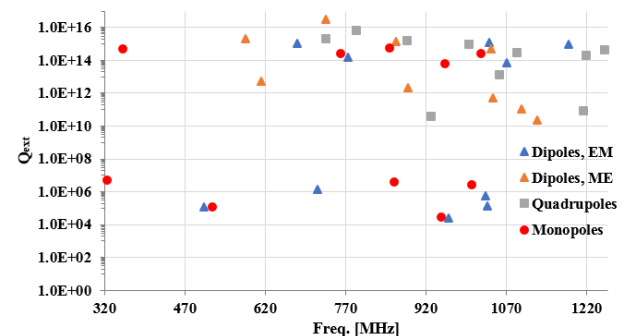


Figure 13: Q_{ext} for SSR2 v3.1 HOMs through the fundamental power coupler.

LORENTZ FORCE DETUNING AND df/dp

Multi-physics simulations have been run with COMSOL which allows easy coupling between mechanics and RF solvers, combined with moving mesh capabilities. The cavity eigen-frequency is calculated first for unperturbed geometry; then either an external pressure is applied to the Helium volume (df/dp) or an electromagnetic pressure is applied to the RF surface (LFD). After the mechanic solver is done computing the displacements, the mesh nodes are updated by the moving mesh solver and the eigen-frequency is recalculated by the RF solver. All displacements have been cross-checked between COMSOL and Ansys, Fig. 14 shows the SR2 v3.1 displacement due to 2.05 bar He pressure. Niobium shell thickness has been set to 3.75 mm. This value

Content from this work may be used under the terms of the CC BY 3.0 licence (© 2019). Any distribution of this work must maintain attribution to the author(s), title of the work, publisher, and DOI.

is obtained from raw Niobium sheet thickness considering the various contributions to its reduction: from the forming process to the final cavity light chemical processing. In [10] a full summary of the mechanical design of the new SSR2 cavity is reported including all consideration for df/dp and LFD and their optimization.

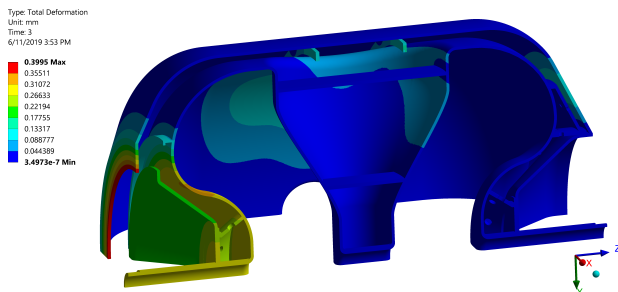


Figure 14: SSR2 v3.1 displacements (in mm) due the 2.05 Bar of He pressure.

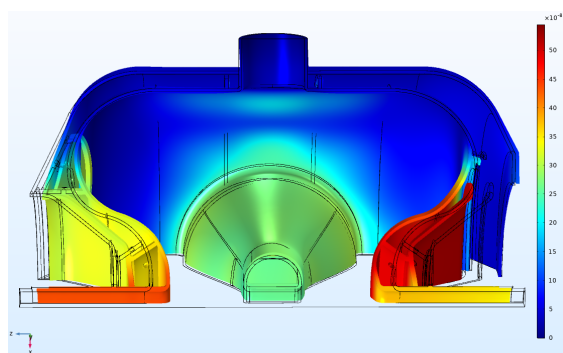


Figure 15: Cavity shell deformation in m under Lorentz pressure calculated at $E_{acc} = 10$ MV/m.

When calculating both LFD and df/dp the tuner stiffness has been taken into account and it has been applied to the cavity beam tube, only where the tuner will be installed. Figure 15 shows the Niobium shell deformation due to Lorentz pressure normalized at $E_{acc} = 10$ MV/m. Magnetic Lorentz pressure is positive, while the electric field contribution is negative. A design optimization of both cavity and He vessel has been performed to minimize LFD coefficient, also taking into account the ease of manufacturing. The tuner stiffness is considered to be 70 kN/mm and corresponds to an LFD coefficient of -3.65 Hz/(MV/m)² requirement for PIP-II is 4 Hz/(MV/m)². For the optimized cavity df/dp value is <1 Hz/mbar — well below the required value (25 Hz/mbar).

CONCLUSION

SSR2 cavity for PIP-II EM design is completed, cavity performance are appropriate for machine operation.

Quadrupole field asymmetry, MP and HOMs have been studied and do not represent an issue. LFD and df/dp have been analyzed and mitigated to guarantee easier cavity operation. Multipacting has been mitigated by modifying the cavity end-wall curvature: the new SSR2 v3.1 shows lower MP intensity than SSR1 cavity already built and tested. The cavity design is now ready for mechanical study and optimization, presented in [10].

REFERENCES

- [1] V. Lebedev, PIP-II RDR, http://pxie.fnal.gov/PIP-II_RDR/
- [2] P. Berrutti, T.N. Khabiboulline, L. Ristori, G.V. Romanov, A.I. Sukhanov, and V.P. Yakovlev, “Multipacting Simulations of SSR2 Cavity at FNAL”, in *Proc. NAPAC'13*, Pasadena, CA, USA, Sep.-Oct. 2013, paper WEPAC23, pp. 838–840.
- [3] P. Berrutti, T.N. Khabiboulline, and V.P. Yakovlev, “Update on SSR2 Cavity EM Design for PIP-II”, in *Proc. LINAC'16*, East Lansing, MI, USA, Sep. 2016, pp. 920–922. doi : 10.18429/JACoW-LINAC2016-THPLR032
- [4] A.I. Sukhanov *et al.*, “Cold Tests of SSR1 Resonators for PXIE”, in *Proc. SRF'13*, Paris, France, Sep. 2013, paper MOP014, pp. 112–116.
- [5] T.N. Khabiboulline *et al.*, “High Gradient Tests of the Fermilab SSR1 Cavity”, in *Proc. IPAC'12*, New Orleans, LA, USA, May 2012, paper WEPPC052, pp. 2330–2332.
- [6] Z.Y. Yao, R.E. Laxdal, B.S. Waraich, V. Zvyagintsev, and R. Edinger, “Study of Balloon Spoke Cavities”, in *Proc. SRF'13*, Paris, France, Sep. 2013, paper THP033, pp. 972–974.
- [7] Z.Y. Yao *et al.*, “Fabrication and Test of $\beta=0.3$ 325 MHz Balloon Single Spoke Resonator”, in *Proc. IPAC'18*, Vancouver, Canada, Apr.-May 2018, pp. 3934–3936. doi : 10.18429/JACoW-IPAC2018-THPAL123
- [8] P. Berrutti, M.H. Awida, I.V. Gonin, N. Solyak, A. Vostrikov, and V.P. Yakovlev, “Optimization of the Geometric Beta for the SSR2 Cavities of the Project X”, in *Proc. IPAC'12*, New Orleans, LA, USA, May 2012, paper WEPPC045, pp. 2312–2314.
- [9] P. Berrutti, T.N. Khabiboulline, V.A. Lebedev, and V.P. Yakovlev, “Transverse Field Perturbation For PIP-II SRF Cavities”, in *Proc. IPAC'15*, Richmond, VA, USA, May 2015, pp. 3302–3305. doi : 10.18429/JACoW-IPAC2015-WEPTY019
- [10] M. Parise, D. Passarelli, F. Ruii, P. Duchesne, D. Longuevergne, and D. Reynet, “Mechanical Design and Fabrication Aspects of Prototype SSR2 Jacketed Cavities”, presented at the SRF'19, Dresden, Germany, Jun.-Jul. 2019, paper TUP014, this conference.